Elevation-dependent compensation effects in snowmelt in the Rhine River Basin upstream gauge Basel

Erwin Rottler, Klaus Vormoor, Till Francke, Michael Warscher, Ulrich Strasser and Axel Bronstert

ABSTRACT

In snow-dominated river basins, floods often occur during early summer, when snowmelt-induced runoff superimposes with rainfall-induced runoff. An earlier onset of seasonal snowmelt as a consequence of a warming climate is often expected to shift snowmelt contribution to river runoff and potential flooding to an earlier date. Against this background, we assess the impact of rising temperatures on seasonal snowpacks and quantify changes in timing, magnitude and elevation of snowmelt. We analyse *in situ* snow measurements, conduct snow simulations and examine changes in river runoff at key gauging stations. With regard to snowmelt, we detect a threefold effect of rising temperatures: snowmelt becomes weaker, occurs earlier and forms at higher elevations. Due to the wide range of elevations in the catchment, snowmelt does not occur simultaneously at all elevations. Results indicate that elevation bands melt together in blocks. We hypothesise that in a warmer world with similar sequences of weather conditions, snowmelt is moved upward to higher elevation. The movement upward the elevation range makes snowmelt in individual elevation bands occur earlier, although the timing of the snowmelt-induced runoff stays the same. Meltwater from higher elevations, at least partly, replaces meltwater from elevations below.

Key words | compensation effects, elevation-dependency, Rhine River, snowmelt, timing

HIGHLIGHTS

- Impact of rising temperatures on seasonal snowpacks.
- Investigations on the point scale for elevation bands and from a catchment perspective.
- *Threefold effect*: snowmelt becomes weaker, occurs earlier and forms at higher elevations.
- Meltwater from higher elevations can, at least partly, replace meltwater from elevations below.

Erwin Rottler (corresponding author)
Klaus Vormoor
Till Francke
Axel Bronstert
Institute of Environmental Science and Geography,
University of Potsdam,
Karl-Liebknecht-Str. 24-25, 14476 Potsdam,
Germany
E-mail: *rottler@uni-potsdam.de*

Michael Warscher
Ulrich Strasser
Department of Geography,
University of Innsbruck,
Innrain 52, 6020 Innsbruck,
Austria

doi: 10.2166/nh.2021.092

GRAPHICAL ABSTRACT

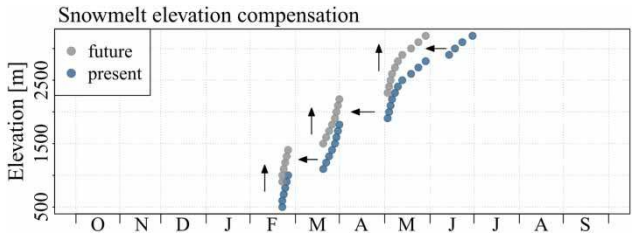

INTRODUCTION

Alpine landscapes react particularly sensitively towards climatic changes. By the end of the century, glaciers in the European Alps most likely will be gone, and seasonal snowpacks downsized to a small fraction (Horton *et al.* 2006; Zemp *et al.* 2006; Huss 2011; Fatichi *et al.* 2014; Gobiet *et al.* 2014; Beniston *et al.* 2018; Hanzer *et al.* 2018). Cryospheric changes are ongoing and will fundamentally alter river runoff and water availability on regional and global scales (Stewart 2009; Clow 2010; Gillan *et al.* 2010; Viviroli *et al.* 2011; Laghari *et al.* 2012; Radić & Hock 2014).

Snowmelt is an important flood-generating process (Berghuijs *et al.* 2019; Parajka *et al.* 2019). In snow-dominated river basins, flooding often occurs during spring and early summer, when high baseflow due to snowmelt overlaps with strong precipitation (Wetter *et al.* 2011; Vormoor *et al.* 2015). For Switzerland, changes in mean and extreme regimes in both rainfall and melt-dominated regions are expected (Addor *et al.* 2014; Brunner *et al.* 2019). Recent studies investigating regional flood discharge trends for Europe indicate that climate change impact on flood timing and frequency is ongoing already (Blöschl *et al.* 2017, 2019; Bertola *et al.* 2020).

Studies analysing cryospheric and hydrological climate change impacts often focus on changes in timing and mean annual cycles in relatively small areas, i.e. individual valleys. Seldom, larger catchments covering a wide range of elevations and pre-alpine to high alpine areas are analysed. So far, only very few studies have resolved changes along the elevation range (e.g. Hunsaker *et al.* 2012; Kormann *et al.* 2015). However, in alpine settings, temperature is a function of both time and elevation. Elevation as an additional dimension with regard to changes in snowmelt often receives only little attention.

In this study, we analyse snow observations, conduct snow simulations and analyse discharge records from key gauging stations in the Rhine Basin upstream gauge Basel. We use Moderate Resolution Imaging Spectrometer (MODIS) snow cover maps to validate our model results. The main goal is to better understand the impact of rising temperatures on alpine snowpacks. We focus on the timing, magnitude and elevation of snowmelt events and assess how changes in snowmelt translate into changes in river runoff.

STUDY AREA AND DATA

The study area is the Rhine Basin upstream gauge Basel. The basin covers a total area of 3.59×10^4 km² and an elevation range of almost 4,000 m (Figure 1). Gauge Basel is located at 294 m a.s.l. The southern parts of the basin are of high-alpine character. The highest mountain peaks reach up to elevations above 4,000 m a.s.l. In winter, precipitation is often solid and accumulates in temporary snowpacks. Depending on the elevation, areas are covered by snow for weeks or even months. A considerable fraction of runoff originates from snowmelt (Stahl *et al.* 2016). In general, elevation is an important factor determining local climatic conditions, vegetation and land use. The basin also encompasses large parts of the Swiss Plateau, hilly to flat areas north of the alpine ridge, which mostly cover elevations between 300 and 1,000 m a.s.l. In recent decades, temperatures in the Swiss Alps have been rising at a very fast pace

(e.g. Ceppi *et al.* 2012; Rottler *et al.* 2019). Studies *inter alia* hint at changes in forest growth, species distribution and phenology (e.g. Walther *et al.* 2005; Gehrig-Fasel *et al.* 2007; Mietkiewicz *et al.* 2017). Very prominent changes have been observed with regard to glaciers (Zemp *et al.* 2006; Huss & Farinotti 2012; Fischer *et al.* 2014; Beniston *et al.* 2018). Strong alteration of runoff due to rising temperatures is expected in glacierized headwater catchments (Huss *et al.* 2008; Junghans *et al.* 2011). However, the importance of ice melt with regard to runoff decreases with the distance to the glacier. At gauge Basel, only 2% of the total annual runoff originates from ice melt (Stahl *et al.* 2016). The investigations presented are based on daily records of temperature, rainfall, snow depth and discharge measurements, MODIS snow cover maps and *in situ* observations of snow water equivalent (SWE), as well as gridded temperature and rainfall datasets.

All station-based meteorological and cryospheric observational data were provided by the Federal Office of Meteorology and Climatology of Switzerland (MeteoSwiss) and the Institute for Snow and Avalanche Research (SLF) from the Swiss Federal Institute for Forest, Snow and Landscape Research (WSL) (Supplementary Table A1). Discharge time series were obtained from the Global Runoff Data Centre (GRDC). Daily and nearly cloud-free MODIS snow cover maps for the European Alps in a resolution of 250 m and from 2002 onwards were provided by the Institute for Earth Observation, Eurac Research, Bolzano/Bozen, Italy (Matiu *et al.* 2019, 2020). All data analysis was carried out using the free software R 3.6.1 (R Core Team 2019).

MeteoSwiss and WSL conduct monitoring and analysis programmes for the snowpack in Switzerland at numerous locations. In this study, we focus on a few selected stations. Selected records of snow depth stand out by their length and cover a broad range of elevations, i.e. 555–2,691 m a.s.l. To examine changes in river runoff, we exert a nested catchment approach in the two main branches of the Rhine River network: the Aare branch (left in Figure 1) and the Rhine branch including Lake Constance (right in Figure 1). The two branches flow together approximately 60 km upstream Basel. The Aare River is the main tributary of the High Rhine. We analyse discharge data from the Aare River recorded at gauges Bern, Brugg and Untersiggenthal. Between gauges Brugg and Untersiggenthal, the two rivers Reuss and Limmat merge with the Aare River increasing the size of the Aare River Basin by about 50%. The Rhine branch is subdivided into nested basins from gauges Diepoldsau, Neuhausen and Rekingen. The enclosing character of individual basins enables the backtracking and localisation of changes in runoff. Gridded temperature and precipitation data used to drive snow simulations originate from E-OBS v12 gridded datasets from the European Climate & Dataset

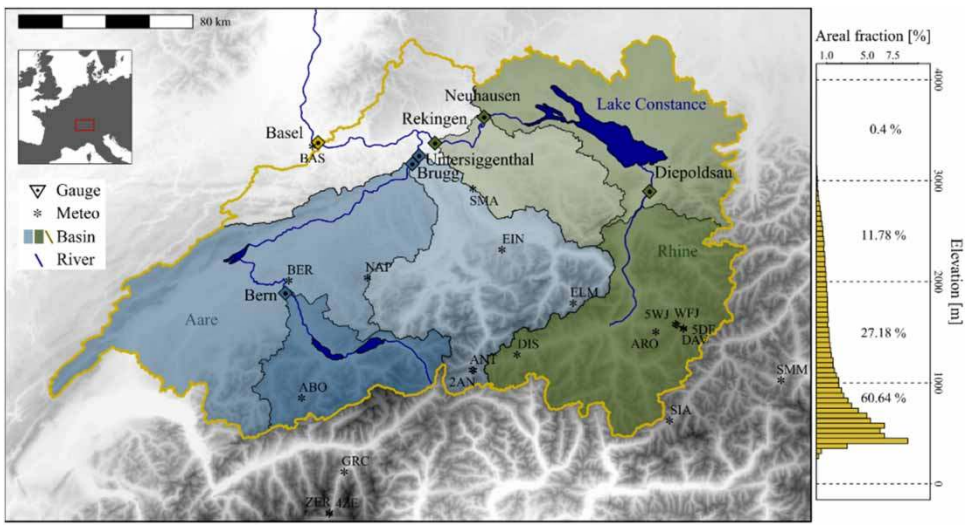

Figure 1 | Topographic map of the Rhine Basin upstream gauge Basel (main map) with locations of meteorological stations and nested catchments of the Aare River (Bern–Brugg–Untersiggenthal; blue) and the Rhine River (Diepoldsau–Neuhausen–Rekingen; green) and elevation distribution of the Rhine Basin until gauge Basel (raster cells in a 500-m resolution based on the EU-DEM v1.1 by the EU Copernicus Programme). Please refer to the online version of this paper to see this figure in colour: http://dx.doi.org/10.2166/nh.2021.092.

(ECA&D) project (Hofstra *et al.* 2008; Cornes *et al.* 2018). Within the project 'EDgE – End-to-end Demonstrator for improved decision making in the water sector in Europe' by Copernicus, these data were further refined to a 5 km grid using external drift kriging (EDK). EDK addresses altitude effects and provides input data for hydrological modelling at high spatial resolutions (e.g. Zink *et al.* 2017; Marx *et al.* 2018; Samaniego *et al.* 2018; Thober *et al.* 2018).

METHODS

Our analysis is based on the combination of both observed and modelled data. We analyse changes in snowpacks and snowmelt dynamics and assess the effect of changes in snowpacks on the timing and magnitude of snowmelt-induced runoff. An in-depth analysis of discharge data and governing flood drivers complements the investigations (Figure 2).

Snow observations

To get a first insight into observed changes in snowpacks, we display snow observations as raster graphs and determine the mean annual cycle for snow depth and accumulation/melt rates for two time windows: 1958–1987 and 1988–2017. We select the time windows in order to have two 30-year windows with maximum data availability at individual stations while keeping a sufficient overlap with the snow simulation period (1951–2014). Enhanced warming since the 1980s strongly affects Swiss snowpacks (Laternser & Schneebeli 2003; Scherrer *et al.* 2004; Marty 2008; Philipona *et al.* 2009; Rottler *et al.* 2019). By comparing two 30-year windows located before and after the onset of strong changes, we aim to capture signals of change in the snow cover in a robust way. Accumulation/melt rates are calculated as the difference in snow depth between two consecutive days. These mean annual cycles are calculated after applying a 30-day moving average window.

Snow simulations: model selection, adaption and verification

We conduct snow simulations in order to extend first insights gained by analysing snow observations. For our study, we need a flexible snow model that is able to easily operate on spatial scales of several thousand square kilometres and time frames of several decades. The main focus is on the effect of changing temperatures on the timing and magnitude of snowmelt events. As rain-on-snow can be an important driver of high melt rates, the energy input from rainfall needs to be represented. In view of the model requirements, we conduct snow simulations using the energy balance method of the modelling framework ECHSE (Eco-Hydrological Simulation Environment) (Kneis 2015). In comparison to empirical approaches, physically based model setups allow more detailed investigations of the snow cover processes and offer several possibilities to refine the model setup if necessary.

ECHSE is an open-source modelling framework developed to facilitate 'the rapid development of new, re-usable simulation tools and, more importantly, the safe modification of existing formulations' (Kneis 2015). The ECHSE environment provides mathematical representations of various hydrological processes, e.g. evapotranspiration, runoff concentration or the dynamics of a snow cover. Recent application of the ECHSE modelling framework includes Abon *et al.* (2016), Kneis *et al.* (2017) and Pilz *et al.* (2020). A key feature of ECHSE is its well-documented open-source software, which forms the basis for transparent and reproducible studies. In our analysis, we do not build an entire model engine but focus on the simulation of the Alpine snow cover. The standard ECHSE snow module couples mass and energy balances with SWE and snow energy content as primary state variables. Snow albedo is considered an auxiliary state variable. The meltwater outflow from the snowpack is computed from available meltwater and the current hydraulic conductivity in the snowpack. A detailed description of the snow module including all equations can be found in Kneis (2014). We use the original functions from the ECHSE online repository written in C++ and conduct simulations in an R environment. To avoid instabilities in the melting process, we perform daily snow simulations in 24 intermediate steps, with daily mean temperature input values being disaggregated assuming sinusoidal diurnal temperature variations. Thereby the amplitude was set to 8 °C, and the timing of the maximum value to 14:00 h. Daily precipitation input is equally distributed among all intermediate time steps. An average yearly cycle

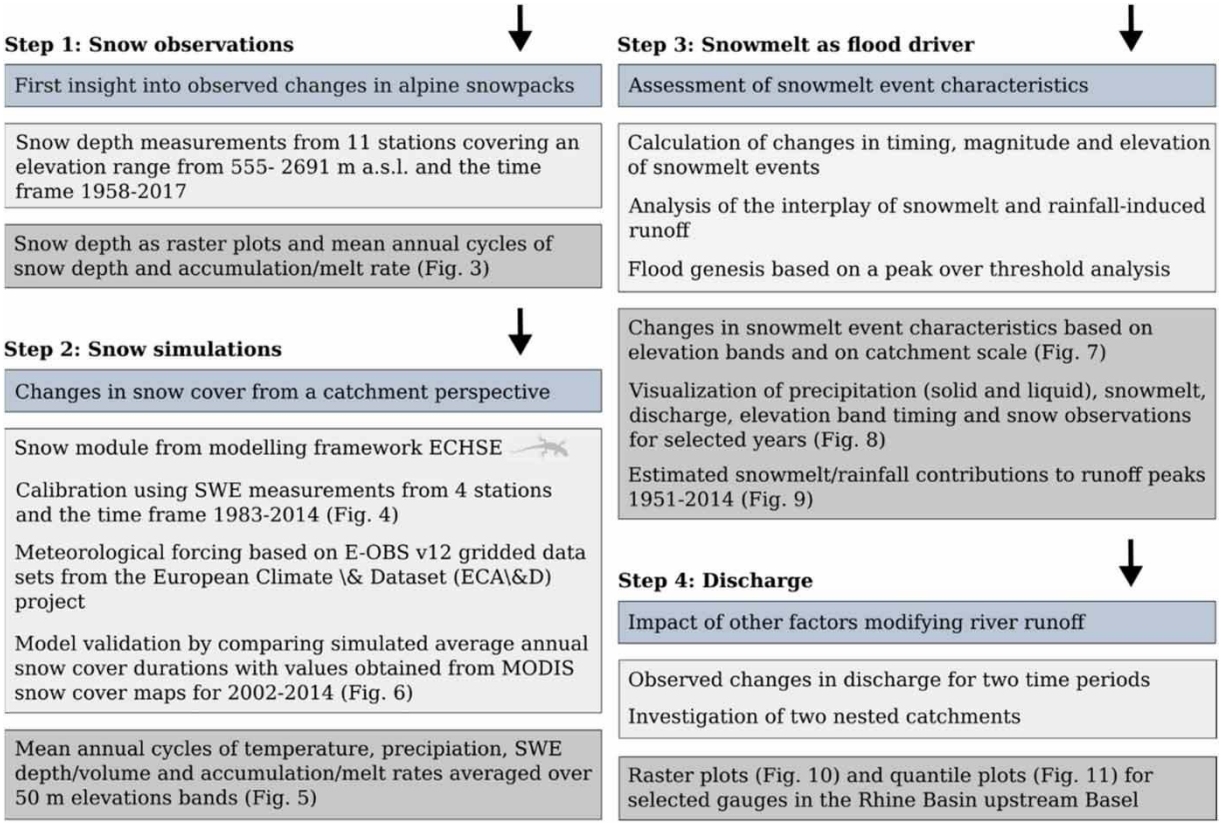

Figure 2 | Schematic overview of analytical steps describing main objective, data, methods and visualisation techniques. Please refer to the online version of this paper to see this figure in colour: http://dx.doi.org/10.2166/nh.2021.092.

of global radiation is calculated based on measurements (1981–2017) from the Swiss meteorological station Napf (1,404 m a.s.l) and used as radiation input. Values of air pressure, relative humidity, wind speed and cloud coverage are currently assumed to be constant with values of 1,000 hPa, 70%, 1 m/s and 50%, respectively.

As a first step, we validate the model setup and modifications using measured temperature and precipitation records from meteorological stations and a default parameter set for daily data from two sites in the German low mountain ranges (Kneis 2014). After ascertaining flawless model operation, we re-calibrate model parameters (see Supplementary Table B1) using the particle swarm optimisation algorithm from the R-package 'ppso' (https://github.com/TillF/ppso). This calibration aims to improve model performance by customising parameters to the alpine setting. We employ 5,000 model runs and assess model performance using the average normalised root-mean-square error (NRMSE) using the standard deviation of the observations (Zambrano-Bigiarini 2017) between simulated and measured SWE for the locations Andermatt, Davos, Zermatt and Weissfluhjoch within the time frame 1983–2014, i.e. the maximum overlap of available meteorological input for snow simulations. We use the NRMSE in the attempt to weight stations equally during calibration. We give the NRMSE in percentage. A value of 100% indicates that the RMSE is equal to the standard deviation. To facilitate the evaluation of attained values, we also calculate the percentage bias (PBIAS) (Sorooshian *et al.* 1993) and the Nash–Sutcliffe Efficiency (NSE) (Nash & Sutcliffe 1970).

Next, we use the resulting parameters and gridded datasets of temperature and precipitation (available for the time frame 1950–2014) to perform snow simulations for the entire study area upstream gauge Basel. The temperature grid used to drive the simulations was obtained by downscaling from 5 to 1 km resolution using a lapse rate-based approach. The lapse rates, i.e. changes of temperature with elevation, were determined every day individually based on

the temperature grid and information on elevation from the EU-DEM v1.1 by the EU Copernicus Programme (resampled to a resolution of 1 km). Based on the information on temperature and elevation, we calculate lapse rates as linear trends using the Theil–Sen trend estimator (Theil 1950; Sen 1968; Bronaugh & Werner 2013). To downscale temperature to the 1-km grid, the temperate lapse rates are multiplied by the elevation differences calculated as the difference between the elevation of the 1 km resolution grid cells and the elevation of the respective cell in the 5-km grid.

In the following, we aggregate results into 50 m elevation bands and calculate annual cycles of mean average and trends in SWE, SWE area volume totals and accumulation/melt rates. Accumulation/melt rates are calculated as the difference in SWE volume between two consecutive days. In addition, we assess mean annual cycles and trends for temperature and precipitation. Trends are determined using the Theil–Sen trend estimator (Theil 1950; Sen 1968; Bronaugh & Werner 2013) after applying a 30-day moving average filter. Grid points showing a continuous accumulation of snow over the simulation period were classified as 'glacier points' and not included in this analysis (2.75% of the data points). To validate our modelling approach, we calculate annual average snow cover durations and compare with satellite-based snow cover maps. With regard to snow simulations, areas are considered covered by snow when SWE is equal to or exceeds 2 mm. All points classified as 'water body' in more than 90% of the MODIS maps were treated as lake surfaces and not included in the analysis.

Snowmelt as flood-driver

Interested in snowmelt as a flood-generating process, we calculate the total snowmelt within a 14-day moving window for all 50 m elevation bands from modelling results, i.e. snowmelt rates, and determine the annual maximum (max14) thereof and assess the two characteristics timing (T-max14) and magnitude (M-max14). In addition, we determine the mean elevation of defined max14 within a 30-day moving window (E-max14). To assess changes over time, we compare max14 characteristics between the two 30-year time frames 1954–1983 and 1984–2013. We also calculate the timing and magnitude of max14 on the catchment scale (T-max14-C and M-max14-C) for the total snow volume in the basin. We assess trend magnitude and significance of these variables using the Theil–Sen trend estimator and the Mann–Kendall trend test (Mann 1945; Kendall 1975).

To improve our understanding of the interplay between snowmelt-induced runoff and rainfall-induced runoff with regard to the annual maximum runoff events, we take a closer look at the 3-day sums of precipitation and 14-day sums of modelled snow accumulation/melt and visualise these variables along with observed discharge measured at gauge Basel. We differentiate between solid and liquid precipitation following the temperature threshold obtained during model calibration (see Supplementary Table B1). In addition, we add information on the timing T-max-14 for all elevation bands to identify elevations contributing most to the snowmelt. Measurements of snow depth from five selected stations are added to enable an additional visual comparison of snowmelt timing in different elevations. We visualise these variables for selected years. We select years with the aim of giving an insight into the different possible interactions between liquid/solid precipitation and the build-up and melt of the seasonal snow cover.

For characterising floods according to their genesis, we use a peak-over-threshold approach: we determine runoff peaks above the 95th percent quantile observed at gauge Basel for the time window 1951–2014 (i.e. time frame of snow simulations). To ensure the independence of detected peaks, two runoff peaks need to be at least 14 days apart. Similar to the approach presented in Vormoor *et al.* (2016), we distinguish rainfall- and snowmelt-driven events by estimating their snowmelt and rainfall contributions based on gridded data. We use the ratio of snowmelt of the preceding 14 days to snowmelt of the preceding 14 days plus liquid precipitation of the preceding 3 days and compare the two time windows 1951–1982 and 1983–2014 for all seasons and for events observed between February and June.

Discharge

In addition to changes in snow cover, many other factors can cause changes in runoff in snow-dominated river basins (e.g. the modification of the river network, the construction and operation of reservoirs of high-head

hydropower plants or changes in precipitation characteristics). The last step of our analysis aims at setting changes in snow cover in relation to other factors. Therefore, we analyse discharge observations for the simulation period 1951–2014 and an extended time frame of 1919–2016. At all gauging stations, continuous daily data are available at least since 1919. The extension of the study period enables the assessment of more robust signals of change less influenced by climate variability. With the aim of getting an overview of runoff seasonality and intra-/inter-annual runoff variability, we display discharge measured as raster graphs (Keim 2000; Koehler 2004). A horizontal line in the figure represents 1 year of measured discharge. Furthermore, we calculate quantile discharge values on a monthly level based on all daily values of a month for the time windows 1951–1982, 1983–2014, 1919–1967 and 1968–2016. These time windows have been chosen to locate two time windows with maximum length in the two time periods investigated, respectively. In the time window 1968–2016, quantiles for the month of January, for example, are based on 49 times 31 daily values. Probability levels investigated range from 0.01 to 0.99. Changes in quantile values between the two investigated time frames are determined by subtracting the value of the older time window from the recent one.

RESULTS

Snow observations

Seasonal snowpack characteristics are subject to strong inter-annual variability (Figure 3(a)). In recent decades (1988–2018), seasonal snowpacks are diminished at all stations compared to 1958–1988 (Figure 3(b)). Our results indicate that accumulation is reduced. The maximum snow depth is often already reached earlier in the year. For stations above 1,000 m, a pattern of increased melt rates at the beginning of the snowmelt period and a reduction in maximum melt rates show up (Figure 3(c)). Snowpacks have already thawed completely earlier in the year. Changes in measured snow depth only are an indication of changes in water stored in the snow cover. During the compaction of a snowpack, for example, snow depth can decrease, while water content stays the same.

Snow simulations: calibration, validation and application of the snowpack model

The snow simulations at the point scale indicate that the calibrated snow model captures the dynamic of high alpine snowpacks well (Figure 4). The average NRMSE of the four stations is 46%, the average PBIAS −5.8% and the NSE 0.78. Both timings of accumulation and melt are in good agreement with observed values. The attained NRMSE indicates that the RMSE is on average less than half a standard deviation of measured values. Furthermore, results indicate that highest SWE values observed at the peak of the snow season tend to be underestimated (e.g. Figure 4(c) and 4(d)). A factor possibly contributing to this uncertainty is a bias in the driving data caused by undercatch of snowfall (Savina *et al.* 2012) and, consequently, reduced precipitation input to the snow simulations.

At the catchment scale, SWE depth and snow cover duration increase with elevation (Figure 5(a)). The total SWE volume is distributed more uniformly along the elevation range, as the areal fraction an elevation band covers decreases with elevation (Figure 1 and 5(c)). Similar to results from snow observations, the simulations indicate that SWE depth and volume is reduced in recent decades, particularly before and during the melt season (Figure 5(b) and 5(d)). We detect a decline also in snow accumulation for elevation bands below approximately 2,000 m. Annual averages and trends in snowmelt/accumulation rates, i.e. snow volume changes between two consecutive days, are depicted in Figure 5(e) and 5(f). The time window where snow is accumulating widens with elevation (Figure 5(e)). At the highest elevation bands investigated, snow is accumulating from October until April. The snowmelt season lasts approximately from February at the lowest elevations to July at the highest elevation.

Negative values in Figure 5(f) indicate either decreases in accumulation or increases in snowmelt (initial negative values further decrease). Positive values in Figure 5(f), on the other hand, indicate either increases in accumulation or decreases in snowmelt. Simulation results hint at an increase in snowmelt at the beginning of the snowmelt period and at an earlier disappearance of the snow at the end of the melting season. For most of the year, decreases in snowmelt rates at the end of the snowmelt season (blue

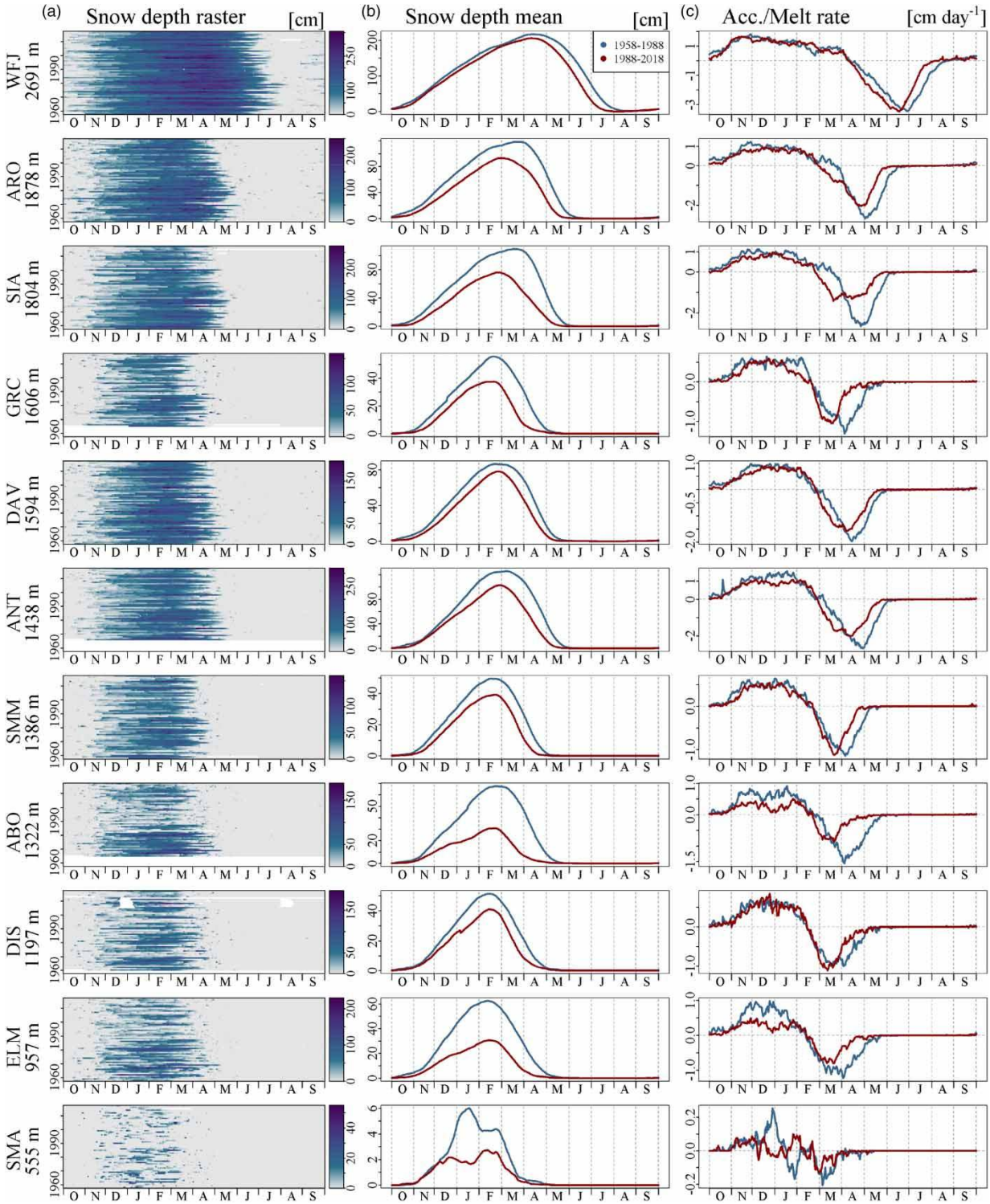

Figure 3 | Snow observation from selected stations for the time frame 1958–2018: (a) snow depth, (b) comparison of mean average annual cycles of snow depth and (c) accumulation/melt rates calculated as the difference in snow depth between two consecutive days for the two 30-year time windows October 1958–September 1988 (blue) and October 1988–September 2018 (red). Mean annual cycles and accumulation/melt rates are computed after applying a 30-day moving average filter. See Supplementary Table A1 for station codes. Please refer to the online version of this paper to see this figure in colour: http://dx.doi.org/10.2166/nh.2021.092.

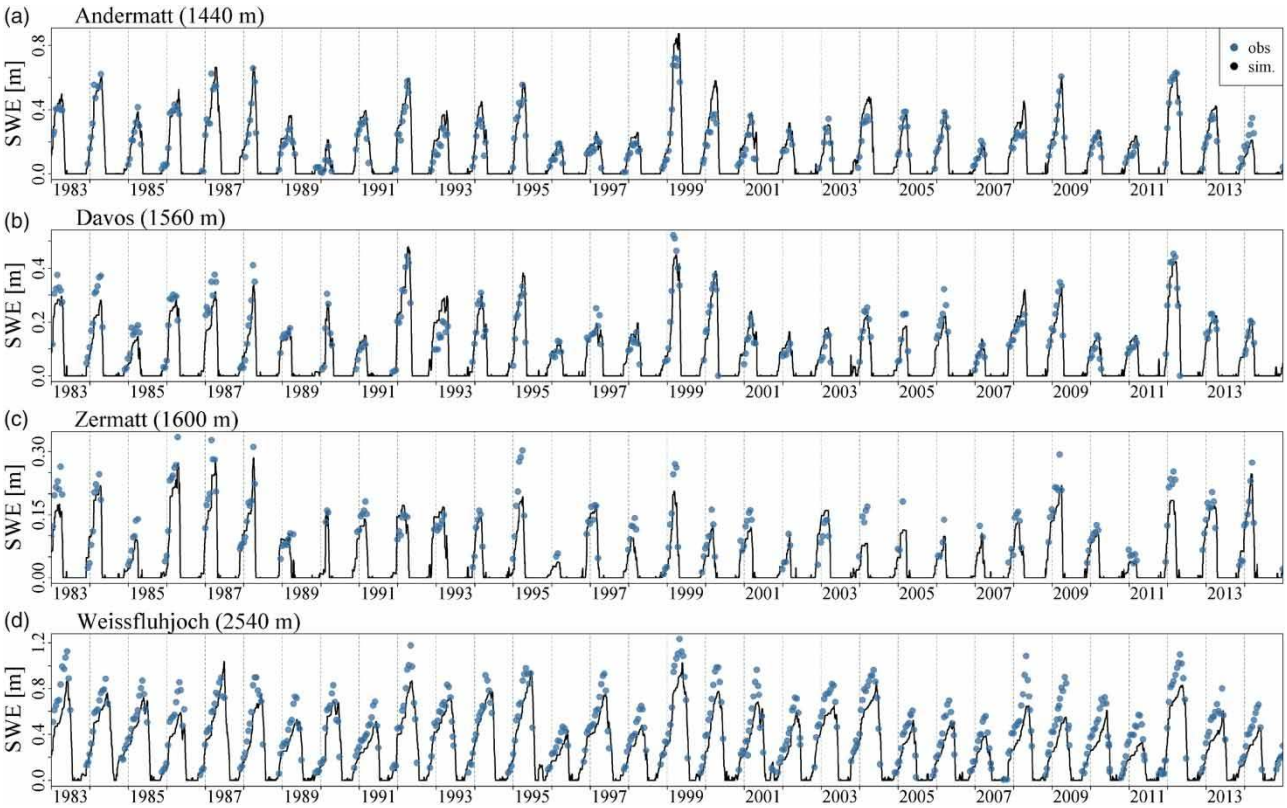

Figure 4 | Simulations and measurements of SWE for stations (a) Andermatt, (b) Davos, (c) Zermatt and (d) Weissfluhjoch. Time frame investigated: 1983–2014. Please refer to the online version of this paper to see this figure in colour: http://dx.doi.org/10.2166/nh.2021.092.

diagonal feature in Figure 5(f)) coincide with increases from higher elevations. In May, for example, snowmelt rates between approximately 1,500 and 2,000 m seem to decrease, while snowmelt rates above 2,000 m increase. Mean annual cycles of average temperatures point at strong differences in temperature depending on elevation and time of the years (Figure 5(g)). Trends in temperature are positive and subject to inter-annual variability (Figure 5(h)). With regard to precipitation, increases and decreases in precipitation show up (Figure 5(h)).

In general, patterns of average annual snow cover duration are similar for simulations and MODIS snow cover maps (Figure 6). The features of the terrain reflect in the duration of the seasonal snow cover. On the Swiss Plateau and on the valley bottoms, there are only few days with snow cover. On the other hand, the high alpine parts are characterised by a short snow-free period. However, differences show up, particularly for two types of areas: (1) in very high elevations, particularly in glaciated areas, satellite-based maps show more days with snow cover and (2) in the valleys of the Alpine Rhine in the South-East, the satellite-based maps show less days with snow cover as compared to the simulation results.

Snowmelt as flood-driver

In recent decades, max14 events occur earlier in the year and are weaker in magnitude (Figure 7(c)). Comparing E-max14 for the two 30-year time frames 1954–1983 and 1984–2013, our results suggest a shift upward the elevation range by about 170 m. On the basin scale, our analysis shows a wide temporal spread of max14 ranging from February to June (Figure 7(c)). No significant change in timing (T-max14-C) nor magnitude (M-max14-C) can be detected.

Figure 8 describes the interplay of precipitation and snowmelt with regard to the annual runoff maximum for four selected hydrological years. In the year 1969/1970, the highest discharge value is observed at the end of February after strong, mainly liquid, precipitation in the basin

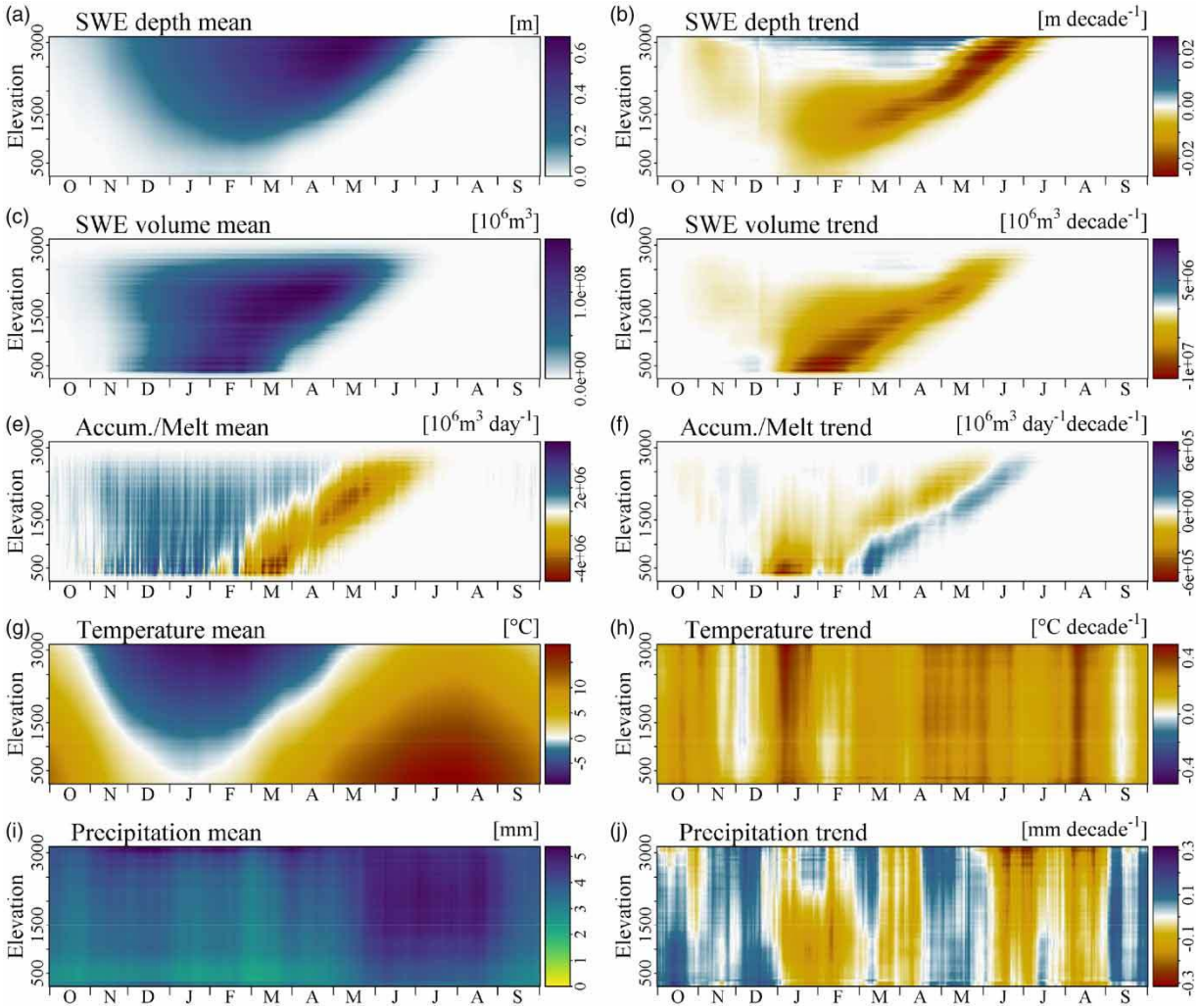

Figure 5 | Snow simulation results for the Rhine basin until gauge Basel for the time frame 1 October 1951–30 September 2014 aggregated to 50 m elevation bands: (a) mean depth SWE, (c) mean SWE volume, (e) mean SWE volume change, i.e. accumulation/melt calculated as the difference in SWE volume between two consecutive days, (g) mean temperature, (i) mean precipitation, (b) trends in SWE depth, (d) trends in mean SWE volume, (f) trends in average daily SWE volume change, (h) trends in temperature and (j) trends in precipitation. Please refer to the online version of this paper to see this figure in colour: http://dx.doi.org/10.2166/nh.2021.092.

(Figure 8(a)). According to the model results, a part of the precipitation input is solid and stored in temporary snowpacks (23%). Our results indicate that the runoff event is exclusively rain-fed, and no snowmelt is contributing. In the year 1978/1979, the annual runoff maximum is recorded in June. Rainfall-induced runoff overlaps with high baseflow due to snowmelt from high elevations (Figure 8(b)). In the two years 1980/1981 and 1987/1988, the annual runoff maximum is recorded in March (Figure 8(c) and 8(d)). In March 1981, strong snowmelt from low elevations overlaps with a moderate rainfall event. In March 1988, heavy precipitation is the main driver of the runoff peak observed. A part of the rainfall is stored in high elevation snowpacks. The temporarily stored water is released in the following months. Snowmelt from low elevations (below 1,000 m a.s.l.), on the other hand, seems to contribute to the observed runoff peak.

In total, we detect 174 independent discharge peaks above the 95th percent quantile at gauge Basel for the time frame 1951–2014 (Figure 9). With regard to the events of all seasons, precipitation is the dominant flood-generating process. Between the months February and June, snowmelt-induced runoff is more important compared with the whole year. Our results indicate that for the time window February and June, 49 out of the 79 detected

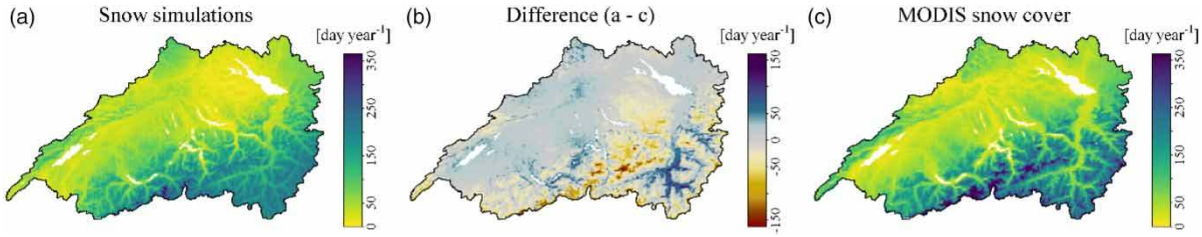

Figure 6 | Average annual snow cover duration (a) simulated and (c) based on daily MODIS snow cover maps (Matiu *et al.* 2020). The difference between (a) and (c) is depicted in (b). Time frame investigated: 1 August 2002–31 July 2014. Please refer to the online version of this paper to see this figure in colour: http://dx.doi.org/10.2166/nh.2021.092.

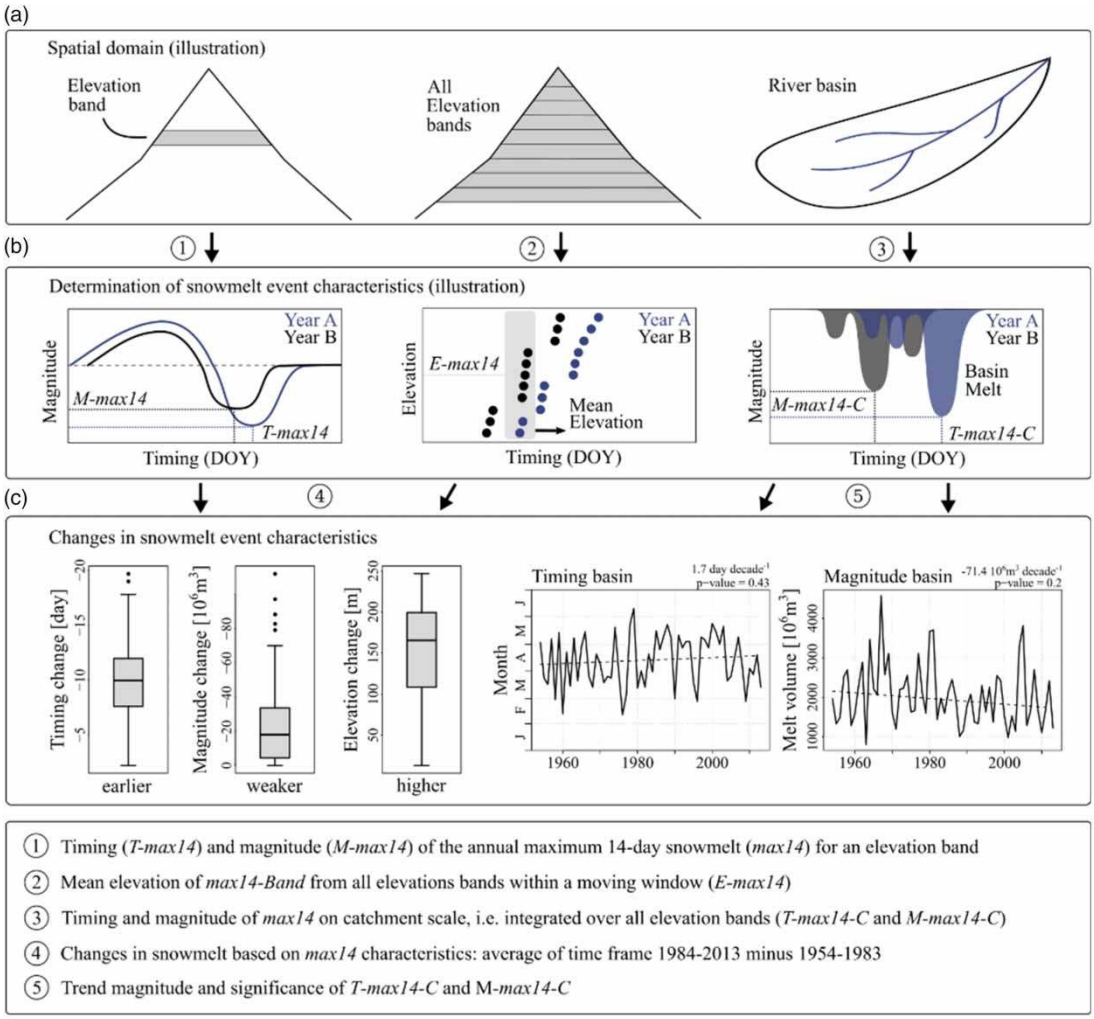

Figure 7 | Determination of snowmelt event characteristics for elevation bands and on catchment scale: (a) spatial domains, (b) illustrations of the determination of snowmelt event characteristics and (c) changes in snowmelt event characteristics based on model simulations. Numbers 1–5 describe analytical steps taken. Please refer to the online version of this paper to see this figure in colour: http://dx.doi.org/10.2166/nh.2021.092.

events for the time frame 1951–2014 potentially have snowmelt contributions of more than 25%. The total number of events and the number of precipitation-dominated events increase in the more recent time frame (1983–2014) with regard to both 'All seasons' and 'February to June'. This overall increase goes along with a decrease in snowmelt contribution to detected events. The number of discharge peaks with potential snowmelt contributions of >50%

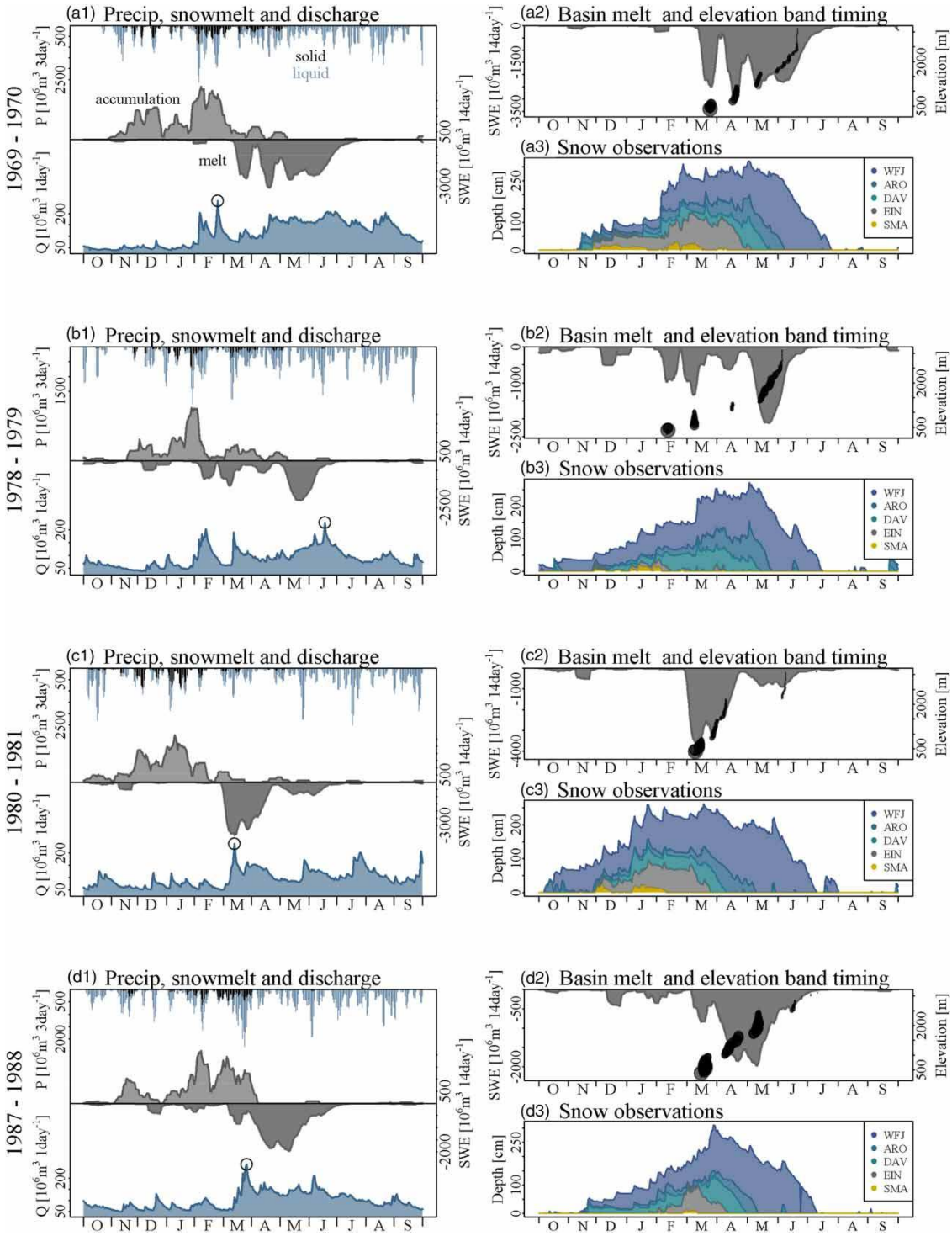

Figure 8 | Simulated snowmelt dynamics and corresponding measured discharge for four selected years in the Rhine Basin until gauge Basel: (1) 3-day moving window sum of precipitation (black/blue indicating solid/liquid precipitation), 14-day moving window sum of snow accumulation/melt (grey) and daily discharge measured at gauge Basel with circles indicating annual runoff maxima, (2) total 14-day moving window sum of snowmelt (grey) with black dots indicating the timing of max14 (point size in proportion to the magnitude of melt event) and (3) snow depth measurements from stations Weissfluhjoch (WFJ – 2,691 m), Arosa (ARO – 1,878 m), Davos (DAV – 1,594 m), Einsiedeln (EIN – 957 m) and Zuerich (SMA – 555 m) (areas between two successive stations coloured according to the higher elevated station). Years displayed: (a) 1969/1970, (b) 1978/1979, (c) 1980/1981 and (d) 1987/1988. Please refer to the online version of this paper to see this figure in colour: http://dx.doi.org/10.2166/nh.2021.092.

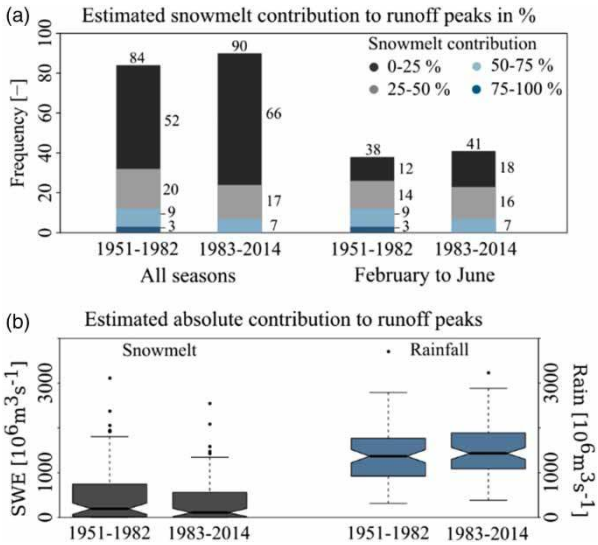

Figure 9 | Frequency of discharge peaks above the 95 percent quantile observed at gauge Basel for the time frame 1951–2014 (two peaks at least 14 days apart): (a) events classified according to the ratio of snowmelt of the preceding 14 days and snowmelt of the preceding 14 days plus precipitation of the preceding 3 days and (b) magnitudes of total 14-day snowmelt and 3-day liquid precipitation preceding the detected runoff peak. Time windows compared: 1951–1982 and 1983–2014. Please refer to the online version of this paper to see this figure in colour: http://dx.doi.org/10.2166/nh.2021.092.

decreases from 12 to 7. Absolute contributions of snowmelt/rainfall tend to decrease/increase (Figure 9(b)).

Discharge

Seasonal snowpacks are an important factor redistributing runoff from winter to summer at all gauges investigated (Figure 10). Runoff seasonality is most pronounced in the alpine part of the catchment (Figure 10(f) and 10(g)). A strong weekly pattern of reservoir operations for hydropower production with higher runoff during weekdays than on the weekend is imprinted at gauge Diepoldsau since the 1960s ('dashed pattern' in Figure 10(g)).

In the Rhine branch including Lake Constance, our results hint at a decrease in runoff during summer (Figure 11(a5)–11(a7) and 11(b5)–11(b7)). At the same time, runoff increases during winter and spring. In the Aare branch including gauges Bern, Brugg and Untersiggenthal, decreases in runoff during the summer seem to be less pronounced (Figure 11(a3) and 11(b1)–11(b3)). The most prominent signal in the Aare branch arises at gauge Brugg: high runoff values increase from the beginning of spring until the beginning of summer (Figure 11(a3) and 11(b3)). At gauge Basel, signals from the two branches overlap, and a general redistribution of runoff from summer to winter superimposes with increases in high runoff values from spring until the beginning of the summer (Figure 11(a1) and 11(b1)). With increasing length of the time windows, patterns showing up get more stable, and differences between neighbouring quantiles and months are less abrupt.

DISCUSSION

Snowmelt event characteristics

Rising temperatures reduce seasonal snowpacks (Figures 3 and 5; Laternser & Schneebeli 2003; Scherrer *et al.* 2004; Marty 2008; Marty & Blanchet 2012; Klein *et al.* 2016). The effects seem most pronounced at elevations below 2,000 m. In those elevations, our simulation results hint at strong decreases during both snow accumulation and snowmelt (Figure 5(b) and 5(d)). In addition, we detect indications of potential elevation-dependent compensation effects for parts of the year (approximately March–June) (Figure 5(f)). Increases/decreases in meltwater outflow seem to be partly compensated by changes in meltwater from the snow cover from elevations below/above. The reduction in seasonal snowpacks goes along with decreases in maximum melt rates (Figure 7(c)). Detected changes go along with results from Musselman *et al.* (2017), who indicate that a 'shallower snowpack melts earlier, and at lower rates, than deeper, later-lying snow-cover' and 'that the fraction of meltwater volume produced at high snowmelt rates is greatly reduced in a warmer climate'.

According to our analysis, rising temperatures do not just decrease the maximum melt rates, we identify a threefold effect: snowmelt becomes weaker, occurs earlier and originates from higher elevations (Figure 7(c)). If we refer to a fixed location (e.g. at an observational site), we can detect the shift forward in time. Conversely, if looking at a fixed time of year, the location of the melt event (i.e. contributing elevation bands) moves upward the elevation range (Figure 12(a)).

Snowmelt as flood-driver

In the Rhine Basin upstream gauge Basel, both snowmelt and precipitation seem to be important flood-drivers. Even moderate precipitation events can cause the annual runoff

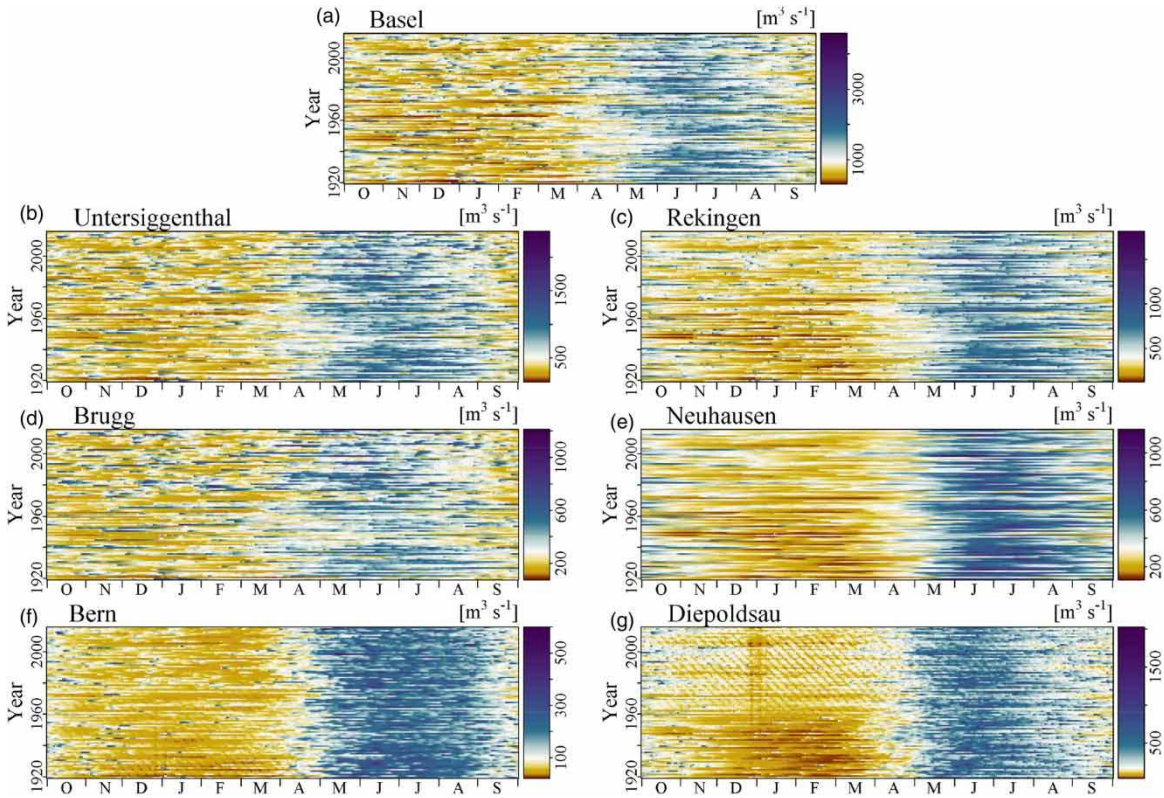

Figure 10 | Raster plots of discharge for the time frame 1919–2016 at river gauges (a) Basel, (b) Untersiggenthal, (c) Rekingen, (d) Brugg, (e) Neuhausen, (f) Bern and (g) Diepoldsau. Left (b, d and f) and right (c, e and g) columns, respectively, represent nested catchments of the Aare and Rhine Rivers, which merge upstream gauge Basel. Please refer to the online version of this paper to see this figure in colour: http://dx.doi.org/10.2166/nh.2021.092.

maximum when superimposing with snowmelt-induced runoff (e.g. Figure 8(c)). Investigations of snow observations and snow simulations demonstrate that snowmelt-induced runoff originates from a wide range of elevations. However, due to this wide elevation range, snowmelt does not occur simultaneously at all elevations. Our results indicate that elevation bands commonly melt together in blocks (Figure 8(a2)–8(d2)). The beginning and end of a snowmelt event occurring in the basin seem to be determined by the passage of warm air masses, the respective elevation range affected by accompanying temperatures and snow availability. We hypothesise that in a warmer climate with similar sequences of weather conditions, snowmelt is moved up to higher elevation, i.e. the block of elevation bands contributing most to the snowmelt-induced runoff is located at higher elevations (Figure 12(b)). The movement upward the elevation range makes snowmelt in individual elevation bands (e.g. T-max14 within an elevation band) occur earlier, and the timing of the snowmelt-induced runoff, however, stays the same. Snowmelt from higher elevation might, at least partly, replace meltwater from lower elevations. Investigating five peak discharge events in the mountain river basin of the Merced River in California, USA, Biggs & Whitaker (2012) were able to show that for each discharge peak, between 60 and 80% of the snowmelt originated from elevations that only covered between 22 and 38% of the total basin relief. They refer to the elevations contributing most to a runoff event as the 'critical zone'.

Role of precipitation

The analysis of the annual runoff maximum of the hydrological year 1969–1970 indicates, in an exemplary way, how precipitation alone can cause high runoff values (Figure 8(a)). According to our analysis, no snowmelt is contributing to the runoff peak. On the contrary, part of the precipitation is solid and stored in temporary snowpacks. The accumulation of snow reduces the effective

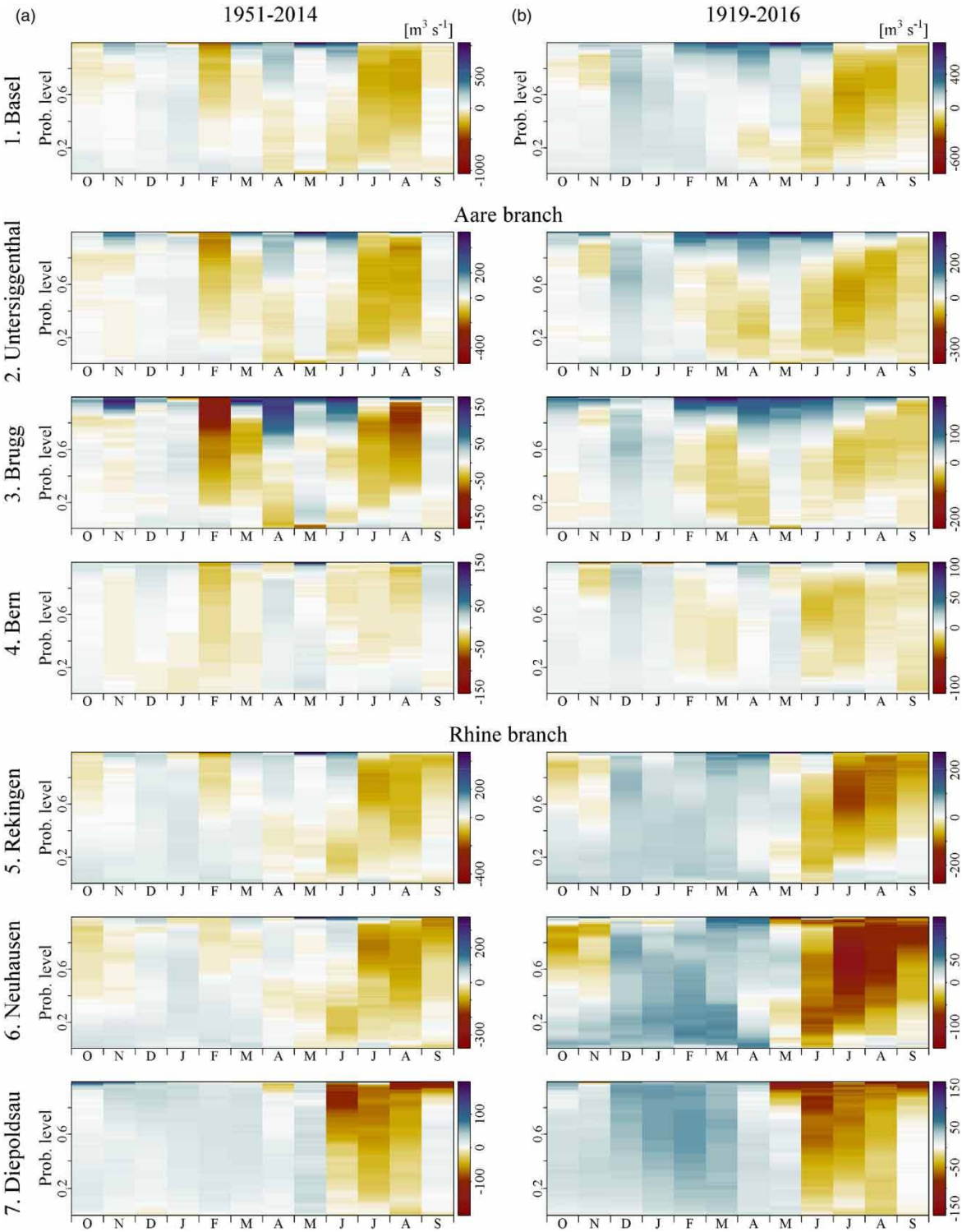

Figure 11 | Change in runoff quantiles from the time window (a) 1951–1982 to 1983–2014 and (b) 1919–1967 to 1968–2016 for probability levels 0.01–0.99 determined with all daily runoff values of a month (quantile value of the earlier time window subtracted from the recent time window). Stations investigated: 1. Basel, 2. Untersiggenthal, 3. Brugg, 4. Bern, 5. Rekingen, 6. Neuhausen and 7. Diepoldsau. Stations 2, 3 and 4 and stations 5, 6, 7, respectively, represent nested catchments of the Aare and Rhine Rivers, which merge upstream gauge Basel. Please refer to the online version of this paper to see this figure in colour: http://dx.doi.org/10.2166/nh.2021.092.

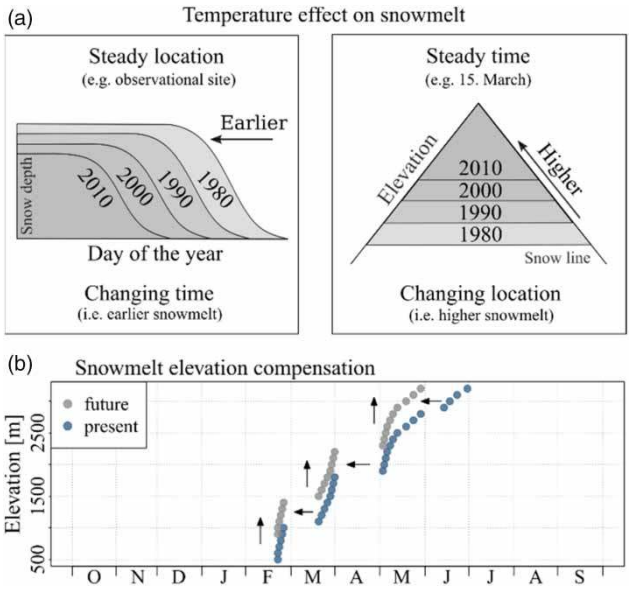

Figure 12 | Idealised effects of rising temperatures on snow cover: (a) earlier and higher snowmelt and (b) idealised change in elevation-dependent contribution to snowmelt with points indicating elevation bands mostly contributing to snowmelt. Arrows indicate shifts forward in time and upward the elevation range, respectively. Please refer to the online version of this paper to see this figure in colour: http://dx.doi.org/10.2166/nh.2021.092.

precipitation, i.e. precipitation translating into river runoff. In the following, we will refer to this effect of partial storage of precipitation in snowpacks as the protective effect of snow accumulation. Strong precipitation events do not have an immediate effect when their water is stored in snowpacks. However, with rising temperatures, the snowline moves upwards and larger fractions of the basin potentially receive liquid precipitation (Barnett *et al.* 2005; Scherrer & Appenzeller 2006; Allamano *et al.* 2009a, 2009b; Kormann *et al.* 2015; Beniston *et al.* 2018). Hence, in a warmer climate, the protective effect of snow accumulation is reduced. Effective precipitation might increase. A simple calculation supports this notion: without the protective effect (all precipitation liquid), the cold season (October until March) annual maxima 3-day rainfall events would have been stronger by 11.4% on average in our simulations. Recent studies point at the increasing importance of rainfall-induced runoff with regard to flooding in catchments influenced by a seasonal snow cover (e.g. Middelkoop *et al.* 2001; Addor *et al.* 2014; Vormoor *et al.* 2016; Brunner *et al.* 2019; Rottler *et al.* 2020). Our analysis of runoff peaks observed at gauge Basel further supports these investigations (Figure 9). The number of runoff peaks with most precipitation as flood-driver tends to increase, while at the same time, events with a majority of snowmelt-induced runoff decrease.

With the analysis of observed discharge, we complete our analysis by assessing changes induced by other factors. The extension of the time frame back to 1919, beyond the simulation period, helps to reduce the impact of inter-annual to decadal climate variability, e.g. due to varying frequencies of weather types (Rottler *et al.* 2019). We attribute detected increases in high runoff values during spring and early summer (Figure 11) to variations in rainfall characteristics. The nested catchment approach indicates that increases in high runoff values during spring and early summer are most prominent at gauge Brugg, whose catchment covers large parts of the Swiss Plateau and whose discharge is most strongly influenced by rainfall-induced runoff compared to the other gauges investigated. Another factor having a strong impact on the runoff in Rhine River Basin upstream gauge Basel are the numerous large reservoirs that have been constructed for hydropower production during the course of the 20th century (e.g. Wildenhahn & Klaholz 1996; Bosshard *et al.* 2013). In the Alpine Rhine Basin until gauge Diepoldsau, for example, the total storage volume is about 10% of the total annual runoff (Bosshard *et al.* 2013). The redistribution of water from summer to winter and a weekly pattern with high/low discharge on weekdays/weekends are well-known effects of reservoir operations (Figure 10(g); Verbunt *et al.* 2005; Belz *et al.* 2007; Meile *et al.* 2011; Pérez Ciria *et al.* 2019; Rottler *et al.* 2020).

Model performance and limitations

We are confident that our modelling approach enables investigations of snow cover changes. Temporal dynamics and absolute values have been reproduced for the stations, patterns realistically generated on the catchment scale. Elevation-dependent differences in snowpack characteristics are represented well. However, our modelling approach includes several assumptions and simplifications that require caution and limit the explanatory value of our simulations. In the framework of our snow model, we do not address changes in incoming solar radiation. Instead, the simple mean annual cycle we use as input *inter alia* does not supply information on recent regional brightening effects (Norris & Wild 2007; Ruckstuhl *et al.* 2008; Ruckstuhl &

Norris 2009; Duethmann & Blöschl 2018). Thus, our modelling setup is solely driven by variations and changes in temperature and precipitation. However, the energy-based concept enables us to address energy input during rain-on-snow events, which is a phenomenon poorly reflected by empirical approaches. Rain-on-snow is an important flood-generating process in upland basins (e.g. Sui & Koehler 2001; Freudiger *et al.* 2014; Rössler *et al.* 2014). The current modelling setup does not include the redistribution of snow by wind or avalanches (e.g. Kerr *et al.* 2013; Warscher *et al.* 2013; Musselman *et al.* 2015; Freudiger *et al.* 2017). Missing redistribution processes increase the uncertainty with regard to snow volume distribution along the elevation range. Furthermore, aspect and slope can be important parameters controlling snow accumulation and snowmelt.

With regard to the detected differences between simulated annual snow cover durations and MODIS snow cover maps, we identify several possible factors contributing to these differences: first, the current model setup does not resolve very high elevations. The resolution of 1 km in combination with the simple lapse rate-based approach to downscale temperature does not capture the highest elevation in the basin. Likewise, it introduces a smoothing effect to the very low-lying cells, resulting in an overestimation of snow cover there. In addition, we suspect that the precipitation input is not capturing the full altitudinal gradient. It seems that climatic conditions, particularly in the valley bottoms in the South-East, are not well captured in the meteorological input used to drive the snow simulations. Precipitation patterns seem too coarse to capture the strong differences over short distances in this complex terrain (Freudiger *et al.* 2016). In addition, the parameters fitted for the observations at the four snow gauges possibly do not capture the entire range of conditions in the basin. Particularly, the snow simulated in the comparatively dry valleys in the South-East and in the highest altitudes might need an adapted set of parameters to describe its properties more accurately.

CONCLUSIONS

We analyse snow and discharge observations and simulate the Alpine snow cover in order to get a better understanding of how changes in snowmelt timing translate into changes in river runoff. The focus of the study is the Rhine River Basin upstream gauge Basel. We are confident that the physically based snow model setup used represents the snow cover dynamics in the basin well. However, several assumptions and simplification advice caution, most importantly the lapse rate-based approaches, applied to downscale gridded temperature input, simple seasonal cycle used as radiation input and the neglect of snow redistribution processes.

Our results point at strong decreases in seasonal snowpacks in recent decades. With regard to snowmelt events, we detect a threefold effect of rising temperatures: snowmelt becomes weaker, occurs earlier and forms at higher elevations (Figure 7(c)). Investigations on the catchment scale indicate that snowmelt-induced runoff can originate from a wide range of elevations. Due to the wide range of elevations covered in the basin, snowmelt does not occur simultaneously at all elevations. Elevation bands rather melt together in blocks (Figure 8). The beginning and end of the release of meltwater seem to be determined by the passage of warm air masses, and the respective elevation range affected by accompanying temperatures and snow availability. We hypothesise that in a warmer world with similar sequences of weather conditions, snowmelt is moved upward to higher elevations, i.e. the block of elevation bands providing most water to the snowmelt-induced runoff is located at higher elevations (Figure 12(b)). The movement upward the elevation range makes snowmelt in individual elevation bands occur earlier, and the timing of the snowmelt-induced runoff, however, stays the same. Meltwater from higher elevations, at least partly, replaces meltwater from elevations below.

Furthermore, our analysis points at the protective effect of snow accumulation with regard to flooding. Precipitation in the form of snow in part of the catchment reduces the effective precipitation, i.e. precipitation directly translating into river runoff. With rising temperatures, the snowline moves upwards and an increased fraction of the precipitation is possibly liquid instead of solid (Scherrer & Appenzeller 2006; Allamano *et al.* 2009b; Vormoor *et al.* 2015). The analysis of discharge time series enabled the assessment of other factors modifying river runoff, i.e. more intense rainfall increasing high runoff quantiles in spring and early summer and the construction of reservoirs for hydropower production redistributing runoff from summer to winter (Meile *et al.* 2011; Bosshard *et al.* 2013; Pérez Ciria *et al.* 2019; Rottler *et al.* 2020).

This study represents a further step towards understanding how changes in alpine snowpacks translate into changes in river runoff. Future studies need to further investigate the proposed hypotheses describing elevation-dependent compensation effects. Investigations using meso-scale hydrological modelling frameworks in combination with satellite data-derived snow cover maps seem predestined for such a task.

ACKNOWLEDGEMENTS

We thank the Federal Office of Meteorology and Climatology of Switzerland (MeteoSwiss), the Institute for Snow and Avalanche Research (SLF) from the Swiss Federal Institute for Forest, Snow and Landscape Research (WSL), the Institute for Earth Observation, Eurac Research and the Global Runoff Data Centre, 56068 Koblenz, Germany (GRDC) for providing meteorological, snow cover and hydrological data, respectively. We acknowledge the datasets generated in the EDgE proof-of-concept project performed under a contract for the Copernicus Climate Change Service (http://edge.climate.copernicus.eu, last accessed: 27 October 2020). ECMWF implements this service and the Copernicus Atmosphere Monitoring Service on behalf of the European Commission.

FUNDING

This research was supported by the Deutsche Forschungsgemeinschaft (GRK 2043/1-P2) within the NatRiskChange research training group at the University of Potsdam.

DATA AVAILABILITY STATEMENT

Data cannot be made publicly available. Readers should contact the corresponding author for details.

REFERENCES

Abon, C. C., Kneis, D., Crisologo, I., Bronstert, A., David, C. P. C. & Heistermann, M. 2016 Evaluating the potential of radar-based rainfall estimates for streamflow and flood simulations in the Philippines. *Geomatics, Natural Hazards and Risk* **7**, 1390–1405. https://doi.org/10.1080/19475705.2015.1058862.

Addor, N., Rössler, O., Köplin, N., Huss, M., Weingartner, R. & Seibert, J. 2014 Robust changes and sources of uncertainty in the projected hydrological regimes of Swiss catchments. *Water Resources Research* **50**, 7541–7562. https://doi.org/10.1002/2014WR015549.

Allamano, P., Claps, P. & Laio, F. 2009a An analytical model of the effects of catchment elevation on the flood frequency distribution. *Water Resources Research* **45**. https://doi.org/10.1029/2007WR006658.

Allamano, P., Claps, P. & Laio, F. 2009b Global warming increases flood risk in mountainous areas. *Geophysical Research Letters* **36**. https://doi.org/10.1029/2009GL041395.

Barnett, T. P., Adam, J. C. & Lettenmaier, D. P. 2005 Potential impacts of a warming climate on water availability in snow-dominated regions. *Nature* **438**, 303–309. https://doi.org/10.1038/nature04141.

Belz, J. U., Brahmer, G., Buiteveld, H., Engel, H., Grabher, R., Hodel, H., Krahe, P., Lammersen, R., Larina, M., Mendel, H.-G., Meuser, A., Müller, G., Plonka, B., Pfister, L. & van Vuuren, W. 2007 *Das Abflussregime Des Rheins Und Seiner Nebenflüsse Im 20. Jahrhundert. Analyse, Veränderungen Und Trends*, Tech. Rep. Bericht Nr. I-22, Internationale Kommission fur die Hydrologie des Rheingebietes (KHR).

Beniston, M., Farinotti, D., Stoffel, M., Andreassen, L. M., Coppola, E., Eckert, N., Fantini, A., Giacona, F., Hauck, C., Huss, M., Huwald, H., Lehning, M., López-Moreno, J.-I., Magnusson, J., Marty, C., Morán-Tejéda, E., Morin, S., Naaim, M., Provenzale, A., Rabatel, A., Six, D., Stötter, J., Strasser, U., Terzago, S. & Vincent, C. 2018 The European mountain cryosphere: a review of its current state, trends, and future challenges. *The Cryosphere* **12**, 759–794. https://doi.org/10.5194/tc-12-759-2018.

Berghuijs, W. R., Harrigan, S., Molnar, P., Slater, L. J. & Kirchner, J. W. 2019 The relative importance of different flood-generating mechanisms across Europe. *Water Resources Research* **55**, 4582–4593. https://doi.org/10.1029/2019WR024841.

Bertola, M., Viglione, A., Lun, D., Hall, J. & Blöschl, G. 2020 Flood trends in Europe: are changes in small and big floods different? *Hydrology and Earth System Sciences* **24**, 1805–1822. https://doi.org/10.5194/hess-24-1805-2020.

Biggs, T. W. & Whitaker, T. M. 2012 Critical elevation zones of snowmelt during peak discharges in a mountain river basin. *Journal of Hydrology* **438–439**, 52–65. https://doi.org/10.1016/j.jhydrol.2012.02.048.

Blöschl, G., Hall, J., Parajka, J., Perdigão, R. A. P., Merz, B., Arheimer, B., Aronica, G. T., Bilibashi, A., Bonacci, O., Borga, M., Canjevac, I., Castellarin, A., Chirico, G. B., Claps, P., Fiala, K., Frolova, N., Gorbachova, L., Gül, A., Hannaford, J., Harrigan, S., Kireeva, M., Kiss, A., Kjeldsen, T. R., Kohnová, S., Koskela, J. J., Ledvinka, O., Macdonald, N., Mavrova-Guirguinova, M., Mediero, L., Merz, R., Molnar,

P., Montanari, A., Murphy, C., Osuch, M., Ovcharuk, V., Radevski, I., Rogger, M., Salinas, J. L., Sauquet, E., Šraj, M., Szolgay, J., Viglione, A., Volpi, E., Wilson, D., Zaimi, K. & Živkovic, N. 2017 Changing climate shifts timing of European floods. *Science* **357**, 588–590. https://doi.org/10.1126/science.aan2506.

Blöschl, G., Hall, J., Viglione, A., Perdigão, R. A. P., Parajka, J., Merz, B., Lun, D., Arheimer, B., Aronica, G. T., Bilibashi, A., Bohác, M., Bonacci, O., Borga, M., Canjevac, I., Castellarin, A., Chirico, G. B., Claps, P., Frolova, N., Ganora, D., Gorbachova, L., Gül, A., Hannaford, J., Harrigan, S., Kireeva, M., Kiss, A., Kjeldsen, T. R., Kohnová, S., Koskela, J. J., Ledvinka, O., Macdonald, N., Mavrova-Guirguinova, M., Mediero, L., Merz, R., Molnar, P., Montanari, A., Murphy, C., Osuch, M., Ovcharuk, V., Radevski, I., Salinas, J. L., Sauquet, E., Šraj, M., Szolgay, J., Volpi, E., Wilson, D., Zaimi, K. & Živkovic, N. 2019 Changing climate both increases and decreases European river floods. *Nature* **573**, 108–111. https://doi.org/10.1038/s41586-019-1495-6.

Bosshard, T., Carambia, M., Goergen, K., Kotlarski, S., Krahe, P., Zappa, M. & Schär, C. 2013 Quantifying uncertainty sources in an ensemble of hydrological climate-impact projections. *Water Resources Research* **49**, 1523–1536. https://doi.org/10.1029/2011WR011533.

Bronaugh, D. & Werner, A. 2013 *Zyp: Zhang + Yue-Pilon Trends Package, R Package Version 0.10-1, Pacific Climate Impacts Consortium*. University of Victoria, Victoria, Canada.

Brunner, M. I., Farinotti, D., Zekollari, H., Huss, M. & Zappa, M. 2019 Future shifts in extreme flow regimes in Alpine regions. *Hydrology and Earth System Sciences* **23**, 4471–4489. https://doi.org/10.5194/hess-23-4471-2019.

Ceppi, P., Scherrer, S. C., Fischer, A. M. & Appenzeller, C. 2012 Revisiting Swiss temperature trends 1959–2008. *International Journal of Climatology* **32**, 203–213. https://doi.org/10.1002/joc.2260.

Clow, D. W. 2010 Changes in the timing of snowmelt and streamflow in Colorado: a response to recent warming. *Journal of Climate* **23**, 2293–2306. https://doi.org/10.1175/2009JCLI2951.1.

Cornes, R. C., van der Schrier, G., van den Besselaar, E. J. M. & Jones, P. D. 2018 An ensemble version of the E-OBS temperature and precipitation data sets. *Journal of Geophysical Research: Atmospheres* **123**, 9391–9409. https://doi.org/10.1029/2017JD028200.

Duethmann, D. & Blöschl, G. 2018 Why has catchment evaporation increased in the past 40 years? A data-based study in Austria. *Hydrology and Earth System Sciences* **22**, 5143–5158. https://doi.org/10.5194/hess-22-5143-2018.

Fatichi, S., Rimkus, S., Burlando, P. & Bordoy, R. 2014 Does internal climate variability overwhelm climate change signals in streamflow? The upper Po and Rhone basin case studies. *Science of The Total Environment* **493**, 1171–1182. https://doi.org/10.1016/j.scitotenv.2013.12.014.

Fischer, M., Huss, M., Barboux, C. & Hoelzle, M. 2014 The New Swiss Glacier Inventory SGI2010: relevance of using high-resolution source data in areas dominated by very small glaciers. *Arctic, Antarctic, and Alpine Research* **46**, 933–945. https://doi.org/10.1657/1938-4246-46.4.933.

Freudiger, D., Kohn, I., Stahl, K. & Weiler, M. 2014 Large-scale analysis of changing frequencies of rain-on-snow events with flood-generation potential. *Hydrology and Earth System Sciences* **18**, 2695–2709. https://doi.org/10.5194/hess-18-2695-2014.

Freudiger, D., Frielingsdorf, B., Stahl, K., Steinbrich, A., Weiler, M., Griessinger, N. & Seibert, J. 2016 Das Potential meteorologischer Rasterdatensätze für die Modellierung der Schneedecke alpiner Einzugsgebiete – potential of meteorological gridded datasets for hydrological modeling in alpine basins. *Hydrologie & Wasserbewirtschaftung* **60**. https://doi.org/10.5675/HyWa_2016,6_1.

Freudiger, D., Kohn, I., Seibert, J., Stahl, K. & Weiler, M. 2017 Snow redistribution for the hydrological modeling of alpine catchments. *WIRES Water* **4**, e1232. https://doi.org/10.1002/wat2.1232.

Gehrig-Fasel, J., Guisan, A. & Zimmermann, N. E. 2007 Tree line shifts in the Swiss Alps: climate change or land abandonment? *Journal of Vegetation Science* **18**, 571–582. https://doi.org/10.1111/j.1654-1103.2007.tb02571.x.

Gillan, B. J., Harper, J. T. & Moore, J. N. 2010 Timing of present and future snowmelt from high elevations in northwest Montana. *Water Resources Research* **46**. https://doi.org/10.1029/2009WR007861.

Gobiet, A., Kotlarski, S., Beniston, M., Heinrich, G., Rajczak, J. & Stoffel, M. 2014 21st century climate change in the European Alps – a review. *Science of the Total Environment* **493**, 1138–1151. https://doi.org/10.1016/j.scitotenv.2013.07.050.

Hanzer, F., Förster, K., Nemec, J. & Strasser, U. 2018 Projected cryospheric and hydrological impacts of 21st century climate change in the Ötztal Alps (Austria) simulated using a physically based approach. *Hydrology and Earth System Sciences* **22**, 1593–1614. https://doi.org/10.5194/hess-22-1593-2018.

Hofstra, N., Haylock, M., New, M., Jones, P. & Frei, C. 2008 Comparison of six methods for the interpolation of daily, European climate data. *Journal of Geophysical Research: Atmospheres* **113**. https://doi.org/10.1029/2008JD010100.

Horton, P., Schaefli, B., Mezghani, A., Hingray, B. & Musy, A. 2006 Assessment of climate-change impacts on alpine discharge regimes with climate model uncertainty. *Hydrological Processes* **20**, 2091–2109. https://doi.org/10.1002/hyp.6197.

Hunsaker, C. T., Whitaker, T. W. & Bales, R. C. 2012 455 snowmelt runoff and water yield along elevation and temperature gradients in California's Southern Sierra Nevada. *JAWRA Journal of the American Water Resources Association* **48**, 667–678. https://doi.org/10.1111/j.1752-1688.2012.00641.x.

Huss, M. 2011 Present and future contribution of glacier storage change to runoff from macroscale drainage basins in Europe. *Water Resources Research* **47**. https://doi.org/10.1029/2010WR010299.

Huss, M. & Farinotti, D. 2012 Distributed ice thickness and volume of all glaciers around the globe. *Journal of Geophysical Research: Earth Surface* **117**. https://doi.org/10.1029/2012JF002523.

Huss, M., Farinotti, D., Bauder, A. & Funk, M. 2008 Modelling runoff from highly glacierized alpine drainage basins in a changing climate. *Hydrological Processes* **22**, 3888–3902.

Junghans, N., Cullmann, J. & Huss, M. 2011 Evaluating the effect of snow and ice melt in an Alpine headwater catchment and further downstream in the River Rhine. *Hydrological Sciences Journal* **56**, 981–993. https://doi.org/10.1080/02626667.2011.595372.

Keim, D. A. 2000 Designing pixel-oriented visualization techniques: theory and applications. *IEEE Transactions on Visualization and Computer Graphics* **6**, 59–78.

Kendall, M. 1975 *Rank Correlation Methods*, 4th edn. Charles Griffin, London.

Kerr, T., Clark, M., Hendrikx, J. & Anderson, B. 2013 Snow distribution in a steep mid-latitude alpine catchment. *Advances in Water Resources* **55**, 17–24. https://doi.org/10.1016/j.advwatres.2012.12.010.

Klein, G., Vitasse, Y., Rixen, C., Marty, C. & Rebetez, M. 2016 Shorter snow cover duration since 1970 in the Swiss Alps due to earlier snowmelt more than to later snow onset. *Climatic Change* **139**, 637–649. https://doi.org/10.1007/s10584-016-1806-y.

Kneis, D. 2014 Eco-Hydrological Simulation Environment (Echse) – Documentation of Model Engines, *Tech. Rep.* Available from: http://echse.github.io/downloads/documentation/echse_engines_doc.pdf (accessed 9 October 2020).

Kneis, D. 2015 A lightweight framework for rapid development of object-based hydrological model engines. *Environmental Modelling & Software* **68**, 110–121. https://doi.org/10.1016/j.envsoft.2015.02.009.

Kneis, D., Abon, C., Bronstert, A. & Heistermann, M. 2017 Verification of short-term runoff forecasts for a small Philippine basin (Marikina). *Hydrological Sciences Journal* **62**, 205–216. https://doi.org/10.1080/02626667.2016.1183773.

Koehler, R. B. 2004 *Raster-Based Analysis and Visualization of Hydrologic Time-Series*. *PhD Thesis*, The University of Arizona.

Kormann, C., Francke, T., Renner, M. & Bronstert, A. 2015 Attribution of high resolution streamflow trends in Western Austria: an approach based on climate and discharge station data. *Hydrology and Earth System Sciences* **19**, 1225–1245. https://doi.org/10.5194/hess-19-1225 2015.

Laghari, A. N., Vanham, D. & Rauch, W. 2012 To what extent does climate change result in a shift in Alpine hydrology? A case study in the Austrian Alps. *Hydrological Sciences Journal* **57**, 103–117. https://doi.org/10.1080/02626667.2011.637040.

Laternser, M. & Schneebeli, M. 2003 Long-term snow climate trends of the Swiss Alps (1931–99). *International Journal of Climatology* **23**, 733–750. https://doi.org/10.1002/joc.912.

Mann, H. B. 1945 Nonparametric tests against trend. *Econometrica* **13**, 245–259. https://doi.org/10.2307/1907187.

Marty, C. 2008 Regime shift of snow days in Switzerland. *Geophysical Research Letters* **35**. https://doi.org/10.1029/2008GL033998.

Marty, C. & Blanchet, J. 2012 Long-term changes in annual maximum snow depth and snowfall in Switzerland based on extreme value statistics. *Climatic Change* **111**, 705–721. https://doi.org/10.1007/s10584-011-0159-9.

Marx, A., Kumar, R., Thober, S., Rakovec, O., Wanders, N., Zink, M., Wood, E. F., Pan, M., Sheffield, J. & Samaniego, L. 2018 Climate change alters low flows in Europe under global warming of 1.5, 2, and 3 °C. *Hydrology and Earth System Sciences* **22**, 1017–1032. https://doi.org/10.5194/hess-22-1017-2018.

Matiu, M., Jacob, A. & Notarnicola, C. 2019 Daily MODIS snow cover maps for the European Alps from 2002 onwards at 250 m horizontal resolution along with a nearly cloud-free version (Version v1.0.2) [data set], Zenodo. https://doi.org/10.5281/zenodo.3601891.

Matiu, M., Jacob, A. & Notarnicola, C. 2020 Daily MODIS snow cover maps for the European Alps from 2002 onwards at 250 m horizontal resolution along with a nearly cloud-free version. *Data* **5** (1). https://doi.org/10.3390/data5010001

Meile, T., Boillat, J.-L. & Schleiss, A. J. 2011 Hydropeaking indicators for characterization of the Upper-Rhone River in Switzerland. *Aquatic Sciences* **73**, 171–182. https://doi.org/10.1007/s00027-010-0154-7.

Middelkoop, H., Daamen, K., Gellens, D., Grabs, W., Kwadijk, J. C., Lang, H., Parmet, B. W., Schädler, B., Schulla, J. & Wilke, K. 2001 Impact of climate change on hydrological regimes and water resources management in the Rhine basin. *Climatic Change* **49**, 105–128. https://doi.org/10.1023/A:1010784727448.

Mietkiewicz, N., Kulakowski, D., Rogan, J. & Bebi, P. 2017 Long-term change in sub-alpine forest cover, tree line and species composition in the Swiss Alps. *Journal of Vegetation Science* **28**, 951–964. https://doi.org/10.1111/jvs.12561.

Musselman, K. N., Pomeroy, J. W., Essery, R. L. H. & Leroux, N. 2015 Impact of windflow calculations on simulations of alpine snow accumulation, redistribution and ablation. *Hydrological Processes* **29**, 3983–3999. https://doi.org/10.1002/hyp.10595.

Musselman, K. N., Clark, M. P., Liu, C., Ikeda, K. & Rasmussen, R. 2017 Slower snowmelt in a warmer world. *Nature Climate Change* **7**, 214–219. https://doi.org/10.1038/nclimate3225.

Nash, J. & Sutcliffe, J. 1970 River flow forecasting through conceptual models Part I – a discussion of principles. *Journal of Hydrology* **10**, 282–290. https://doi.org/https://doi.org/10.1016/0022-1694(70)90255-6.

Norris, J. R. & Wild, M. 2007 Trends in aerosol radiative effects over Europe inferred from observed cloud cover, solar 'dimming,' and solar 'brightening'. *Journal of Geophysical Research: Atmospheres* **112**. https://doi.org/10.1029/2006JD007794.

Parajka, J., Bezak, N., Burkhart, J., Hauksson, B., Holko, L., Hundecha, Y., Jenicek, M., Krajcí, P., Mangini, W., Molnar, P.,

Riboust, P., Rizzi, J., Sensoy, A., Thirel, G. & Viglione, A. 2019 Modis snowline elevation changes during snowmelt runoff events in Europe. *Journal of Hydrology and Hydromechanics* **67**, 101–109. https://doi.org/10.2478/johh-2018-0011.

Pérez Ciria, T., Labat, D. & Chiogna, G. 2019 Detection and interpretation of recent and historical streamflow alterations caused by river damming and hydropower production in the Adige and Inn river basins using continuous, discrete and multiresolution wavelet analysis. *Journal of Hydrology* **578**, 124021. https://doi.org/10.1016/j.jhydrol.2019.124021.

Philipona, R., Behrens, K. & Ruckstuhl, C. 2009 How declining aerosols and rising greenhouse gases forced rapid warming in Europe since the 1980s. *Geophysical Research Letters* **36**. https://doi.org/10.1029/2008GL036350.

Pilz, T., Francke, T., Baroni, G. & Bronstert, A. 2020 How to tailor my process-based hydrological model? Dynamic identifiability analysis of flexible model structures. *Water Resources Research* **56**, e2020WR028042. https://doi.org/10.1029/2020WR028042.

Radic, V. & Hock, R. 2014 Glaciers in the earth's hydrological cycle: assessments of glacier mass and runoff changes on global and regional scales. *Surveys in Geophysics* **35**, 813–837. https://doi.org/10.1007/s10712-013-9262-y.

R Core Team 2019 *R: A Language and Environment for Statistical Computing*. R Foundation for Statistical Computing, Vienna, Austria. Available from: https://www.R-project.org (accessed 9 October 2020).

Rössler, O., Froidevaux, P., Börst, U., Rickli, R., Martius, O. & Weingartner, R. 2014 Retrospective analysis of a nonforecasted rain-onsnow flood in the Alps – a matter of model limitations or unpredictable nature? *Hydrology and Earth System Sciences* **18**, 2265–2285. https://doi.org/10.5194/hess-18-2265-2014.

Rottler, E., Kormann, C., Francke, T. & Bronstert, A. 2019 Elevation-dependent warming in the Swiss Alps 1981–2017: features, forcings and feedbacks. *International Journal of Climatology* **39**, 2556–2568. https://doi.org/10.1002/joc.5970.

Rottler, E., Francke, T., Bürger, G. & Bronstert, A. 2020 Long-term changes in central European river discharge for 1869–2016: impact of changing snow covers, reservoir constructions and an intensified hydrological cycle. *Hydrology and Earth System Sciences* **24**, 1721–1740. https://doi.org/10.5194/hess-24-1721-2020.

Ruckstuhl, C. & Norris, J. R. 2009 How do aerosol histories affect solar 'dimming' and 'brightening' over Europe?: IPCC-AR4 models versus observations. *Journal of Geophysical Research: Atmospheres* **114**. https://doi.org/10.1029/2008JD011066.

Ruckstuhl, C., Philipona, R., Behrens, K., Coen, M. C., Dürr, B., Heimo, A., Mätzler, C., Nyeki, S., Ohmura, A., Vuilleumier, L., Weller, M., Wehrli, C. & Zelenka, A. 2008 Aerosol and cloud effects on solar brightening and the recent rapid warming. *Geophysical Research Letters* **35**. https://doi.org/10.1029/2008GL034228.

Samaniego, L., Thober, S., Kumar, R., Wanders, N., Rakovec, O., Pan, M., Zink, M., Sheffield, J., Wood, E. F. & Marx, A. 2018 Anthropogenic warming exacerbates European soil moisture droughts. *Nature Climate Change* **8**, 421. https://doi.org/10.1038/s41558-018-0138-5.

Savina, M., Schäppi, B., Molnar, P., Burlando, P. & Sevruk, B. 2012 Comparison of a tipping-bucket and electronic weighing precipitation gage for snowfall. *Atmospheric Research* **103**, 45–51. Special Issue on Rainfall in the urban context: forecasting, risk and climate change. https://doi.org/10.1016/j.atmosres.2011.06.010.

Scherrer, S. C. & Appenzeller, C. 2006 Swiss Alpine snow pack variability: major patterns and links to local climate and large-scale flow. *Climate Research* **32**, 187–199. https://doi.org/10.3354/cr032187.

Scherrer, S. C., Appenzeller, C. & Laternser, M. 2004 Trends in Swiss Alpine snow days: the role of local- and large-scale climate variability. *Geophysical Research Letters* **31**. https://doi.org/10.1029/2004GL020255.

Sen, P. K. 1968 Estimates of the regression coefficient based on Kendall's Tau. *Journal of the American Statistical Association* **63**, 1379–1389. https://doi.org/10.1080/01621459.1968.10480934.

Sorooshian, S., Duan, Q. & Gupta, V. K. 1993 Calibration of rainfall-runoff models: application of global optimization to the Sacramento soil moisture accounting model. *Water Resources Research* **29**, 1185–1194. https://doi.org/10.1029/92WR02617.

Stahl, K., Weiler, M., Kohn, I., Freudiger, D., Seibert, J., Vis, M., Gerlinger, K. & Böhm, M. 2016 *The Snow and Glacier Melt Components of Streamflow of the River Rhine and Its Tributaries Considering the Influence of Climate Change*. Synthesis Report I-25, International Commission for the Hydrology of the Rhine Basin, Lelystad, the Netherlands. Available from: https://chr-khr.org/en/file/1057/download?token=Zg6SY04i (accessed 9 October 2020).

Stewart, I. T. 2009 Changes in snowpack and snowmelt runoff for key mountain regions. *Hydrological Processes* **23**, 78–94. https://doi.org/10.1002/hyp.7128.

Sui, J. & Koehler, G. 2001 Rain-on-snow induced flood events in Southern Germany. *Journal of Hydrology* **252**, 205–220. https://doi.org/10.1016/S0022-1694(01)00460-7.

Theil, H. 1950 A rank-invariant method of linear and polynomial regression analysis. *Proceedings of the National Academy of Sciences* **53**. Part I: 386–392, Part II: 521–525, Part III: 1397–1412.

Thober, S., Kumar, R., Wanders, N., Marx, A., Pan, M., Rakovec, O., Samaniego, L., Sheffield, J., Wood, E. F. & Zink, M. 2018 Multi-model ensemble projections of European river floods and high flows at 1.5, 2, and 3 degrees global warming. *Environmental Research Letters* **13**, 014003. https://doi.org/10.1088/1748-9326/aa9e35.

Verbunt, M., Zwaaftink, M. & Gurtz, J. 2005 The hydrologic impact of land cover changes and hydropower stations in the Alpine Rhine basin. *Ecological Modelling* **187**, 71–84. Special

Issue on Advances in Sustainable River Basin Management. https://doi.org/10.1016/j.ecolmodel.2005.01.027.

Viviroli, D., Archer, D. R., Buytaert, W., Fowler, H. J., Greenwood, G. B., Hamlet, A. F., Huang, Y., Koboltschnig, G., Litaor, M. I., LópezMoreno, J. I., Lorentz, S., Schädler, B., Schreier, H., Schwaiger, K., Vuille, M. & Woods, R. 2011 Climate change and mountain water resources: overview and recommendations for research, management and policy. *Hydrology and Earth System Sciences* **15**, 471–504. https://doi.org/10.5194/hess-15-471-2011.

Vormoor, K., Lawrence, D., Heistermann, M. & Bronstert, A. 2015 Climate change impacts on the seasonality and generation processes of floods: projections and uncertainties for catchments with mixed snowmelt/rainfall regimes. *Hydrology and Earth System Sciences* **19**, 913–931. https://doi.org/10.5194/hess-19-913-2015.

Vormoor, K., Lawrence, D., Schlichting, L., Wilson, D. & Wong, W. K. 2016 Evidence for changes in the magnitude and frequency of observed rainfall vs. snowmelt driven floods in Norway. *Journal of Hydrology* **538**, 33–48. https://doi.org/10.1016/j.jhydrol.2016.03.066.

Walther, G.-R., Beißner, S. & Burga, C. A. 2005 Trends in the upward shift of alpine plants. *Journal of Vegetation Science* **16**, 541–548. https://doi.org/10.1111/j.1654-1103.2005.tb02394.x.

Warscher, M., Strasser, U., Kraller, G., Marke, T., Franz, H. & Kunstmann, H. 2013 Performance of complex snow cover descriptions in a distributed hydrological model system: a case study for the high Alpine terrain of the Berchtesgaden Alps. *Water Resources Research* **49**, 2619–2637. https://doi.org/10.1002/wrcr.20219.

Wetter, O., Pfister, C., Weingartner, R., Luterbacher, J., Reist, T. & Trösch, J. 2011 The largest floods in the high Rhine Basin since 1268 assessed from documentary and instrumental evidence. *Hydrological Sciences Journal* **56**, 733–758. https://doi.org/10.1080/02626667.2011.583613.

Wildenhahn, E. & Klaholz, U. 1996 *Große Speicherseen Im Einzugsgebiet Des Rheins*. Tech. Rep. Bericht Nr. II-10, Internationale Kommission fur die Hydrologie des Rheingebietes (KHR), Koblenz.

Zambrano-Bigiarini, M. 2017 *Goodness-of-fit Functions for Comparison of Simulated and Observed Hydrological Time Series*. R Package Version 0.3-10. https://doi.org/10.5281/zenodo.840087. Available from: http://hzambran.github.io/hydroGOF/ (accessed 9 October 2020).

Zemp, M., Haeberli, W., Hoelzle, M. & Paul, F. 2006 Alpine glaciers to disappear within decades?. *Geophysical Research Letters* **33**. https://doi.org/10.1029/2006GL026319.

Zink, M., Kumar, R., Cuntz, M. & Samaniego, L. 2017 A high-resolution dataset of water fluxes and states for Germany accounting for parametric uncertainty. *Hydrology and Earth System Sciences* **21**, 1769–1790. https://doi.org/10.5194/hess-21-1769-2017.

First received 2 June 2020; accepted in revised form 20 December 2020. Available online 20 January 2021